Explaining pulsar timing array observations with primordial gravitational waves in parity-violating gravity

Chengjie Fu,[1,*] Jing Liu,[2,3,†] Xing-Yu Yang,[4,‡] Wang-Wei Yu,[5,6,§] and Yawen Zhang[1]

[1]*Department of Physics, Anhui Normal University, Wuhu, Anhui 241002, China*
[2]*International Centre for Theoretical Physics Asia-Pacific, University of Chinese Academy of Sciences, Beijing 100190, China*
[3]*Taiji Laboratory for Gravitational Wave Universe (Beijing/Hangzhou), University of Chinese Academy of Sciences, Beijing 100049, China*
[4]*Quantum Universe Center (QUC), Korea Institute for Advanced Study, Seoul 02455, Republic of Korea*
[5]*CAS Key Laboratory of Theoretical Physics, Institute of Theoretical Physics, Chinese Academy of Sciences, Beijing 100190, China*
[6]*School of Physical Sciences, University of Chinese Academy of Sciences, Beijing 100049, China*

(Received 14 September 2023; accepted 28 February 2024; published 18 March 2024)

The pulsar timing array (PTA) collaborations have recently suggested the presence of a gravitational wave background at nano-Hertz frequencies. In this paper, we explore potential inflationary interpretation of this signal within the context of a simple and health parity-violating gravity model termed the Nieh-Yan modified teleparallel gravity. Through this model, two inflationary scenarios are evaluated, both yielding significant polarized primordial gravitational waves (PGWs) that align well with the results from PTA observations. Furthermore, the resulting PGWs can display strong circular polarization and significant anisotropies in the PTA frequency band, which are distinct features to be verified by observations of both PTA and the cosmic microwave background. The detection of such a distinctive background of PGWs is expected to provide strong evidence supporting our scenarios and insights into inflationary dynamics and gravity theory.

DOI: 10.1103/PhysRevD.109.063526

I. INTRODUCTION

Inflation is a successful model of the very early Universe that solves the flatness and horizon problems and sets the initial conditions of big bang cosmology. During inflation, the Universe undergoes a period of exponential expansion, during which curvature perturbations from quantum fluctuations of the scalar modes successfully explain the temperature anisotropies in the cosmic microwave background (CMB) and seed the large-scale structure. Primordial gravitational waves (PGWs) are unique prediction of inflation, and detecting them has been considered as a smoking gun for inflation. However, PGWs have yet to be discovered, despite decades of searches in B-mode polarizations in the CMB. The latest constraint on the tensor-to-scalar ratio is obtained by the combination of Planck and BICEP/Keck, with $r < 0.036$ at the 95% confidence level [1]. Apart from observations at the CMB scales, other gravitational wave observation programs, such as the LIGO-Virgo-KAGRA collaboration [2], LISA/Taiji/Tianqin [3–5], and pulsar timing array (PTA) experiments [6–9], offer opportunities to observe PGWs at small scales with modified gravity models or nonstandard thermal histories of the Universe.

Recently, the PTA experiments, including NANOGrav [6], PPTA [7], EPTA [8], and CPTA [9], collectively reported an exciting discovery of nano-Hertz stochastic gravitational wave background (SGWB). Beyond the standard astrophysical interpretation in terms of inspiraling supermassive black hole binaries [10–13], an SGWB stemming from cosmological sources may serve as a potential explanation of the observed signal. This breakthrough promises transformative insights into early universe cosmology. Cosmological SGWBs are expected to originate from vacuum fluctuations or particle production during inflation [14–28], as well as from large primordial scalar perturbations produced during inflation [29–46], cosmological first-order phase transitions [47–51], and topological defects such as cosmic strings [52–54] and domain walls [52,55,56]. A comprehensive review can be found in [57]. The SGWBs originating from these assorted sources have been extensively examined as plausible interpretations of the PTA signal [58–74]. In this study, we concentrate on the vacuum fluctuations during inflation, namely PGWs, exploring the inflationary explanation of the PTA signal within the context of the parity-violating gravity theory.

*fucj@ahnu.edu.cn
†liujing@ucas.ac.cn
‡xingyuyang@kias.re.kr
§yuwangwei@mail.itp.ac.cn

Chern-Simons theory [75,76] is the most widely discussed parity-violating theory of modified gravity. It has been used to generate polarized PGWs [77–82]. However, Chern-Simons theory suffers from ghost instabilities induced by higher-order derivative terms, which have been addressed in more complex models [83–85].

In this work, we investigate a novel modified gravity model that allows for the amplification and observation of PGWs with strong circular polarization, and even large anisotropies. We consider a simple and healthy gravity theory with parity violation [86,87], where the parity symmetry is violated by introducing the scalar field coupled Nieh-Yan term into the teleparallel equivalent of general relativity. Given teleparallel equivalent of general relativity is dynamically equivalent to general relativity (GR), this is equivalently making a parity-violating extension to GR. The first constraint on this model was conducted in [88] through utilizing observational data from LIGO-Virgo GW events. Reference [89] studied the behavior of GWs from this parity-violating gravity model propagating in a medium of collisionless particles. The implications that the Nieh-Yan modified teleparallel gravity (NYmTG) model holds in the context of inflation have been scrutinized in prior work [90], which suggests that the anticipated energy spectrum of PGW signal exhibits a significant bump at frequencies nestled within the range perceptible by prospective GW experiments, surpassing their sensitivity curves. Consequently, it is plausible to infer that the emergent PGWs within the NYmTG model could provide a satisfactory explanation for the PTA signal.

In our scenario, the coupled scalar field acts as either an inflaton or a spectator field with its dynamics during inflation triggering the amplification of PGWs. Such amplified GWs can adequately explain the PTA data. Since the gravitational sources after inflation are constrained by other observables, such as upper bounds on small-scale curvature perturbations [91–93] and observations of GWs at other frequency bands [94,95], PGWs as a product of inflation can safely avoid these constraints and become a promising candidate for cosmological SGWBs to explain the PTA signal. Moreover, this model predicts a characteristic SGWB with simultaneously large anisotropies and large polarization. Since the polarization of an isotropic SGWB cannot be detected by PTA experiments [96,97], this work provides a good opportunity to test both inflation and parity-violating modified gravity model with PTA experiments in the near future.

Throughout the paper, we will use the units $c = \hbar = 1$, the reduced Planck mass $M_{\rm P} = 1/\sqrt{8\pi G} = 1$, and the convention for the metric signature $(+,-,-,-)$.

II. MODEL

We briefly revisit the foundational formulas intrinsic to the NYmTG model, which is characterized by the following action [86,87],

$$S = \int d^4x\sqrt{-g}\left[-\frac{R}{2}+\frac{\alpha\phi}{4}\mathcal{T}_{A\mu\nu}\tilde{\mathcal{T}}^{A\mu\nu}+\frac{1}{2}\nabla_\mu\phi\nabla^\mu\phi-V(\phi)\right] + S_{\rm other}, \tag{1}$$

where R is the Ricci scalar, $\tilde{\mathcal{T}}^{A\mu\nu} = (1/2)\epsilon^{\mu\nu\rho\sigma}\mathcal{T}^{A}{}_{\rho\sigma}$ represents the dual of the torsion two form $\mathcal{T}^{A}{}_{\mu\nu}$ with $\epsilon^{\mu\nu\rho\sigma}$ being the Levi-Civita tensor, and α is the coupling constant. Here, the ϕ field emerges as a dynamical scalar field, and the action $S_{\rm other}$ describes an additional canonical field that is minimally coupled to gravity. With the spatially flat FLRW metric, the background evolution is identical to that in GR, governed by the following equations:

$$3H^2 = \frac{1}{2}\dot{\phi}^2 + V(\phi) + \rho, \tag{2a}$$

$$\ddot{\phi} + 3H\dot{\phi} + \frac{dV}{d\phi} = 0, \tag{2b}$$

$$\dot{\rho} + 3H(\rho + p) = 0, \tag{2c}$$

where H is the Hubble parameter and a dot denotes the derivative with respect to the cosmic time. Here, ρ and p denote the energy density and pressure, respectively, associated with the additional field. It is worth noting that in this model, gauge invariant scalar perturbations corresponding to ϕ vanishes completely due to the coupling of the ϕ field with the Nieh-Yan term. Consequently, if the ϕ field serves as the inflaton, it cannot generate the primordial scalar perturbations. The curvaton scenario, which explains the origin of primordial scalar perturbations in the context of the ϕ field acting as an inflaton, has been thoroughly analyzed in [90].

In this model, the tensor perturbations exhibit the phenomenon of velocity birefringence, obeying the following equation of motion in the momentum space,

$$\ddot{h}^A_k + 3H\dot{h}^A_k + \frac{k}{a}\left(\frac{k}{a} + \lambda_A\alpha\dot{\phi}\right)h^A_k = 0, \tag{3}$$

where $A = R(L)$ denotes the right(left)-handed polarization with $\lambda_R = 1$ and $\lambda_L = -1$. A salient characteristic of the tensor perturbation within this context is the occurrence of tachyonic instability in one of its two polarization states under particular circumstances. For instance, during inflation, there invariably exists a polarization state where the frequency squared of the corresponding modes, denoted by $(k/a)(k/a + \lambda_A\alpha\dot{\phi})$, becomes negative as the physical wave number k/a evolves to be less than $|\alpha\dot{\phi}|$. If the condition $|\alpha\dot{\phi}| > \mathcal{O}(H)$ is met, certain mode functions h^A_k will experience a tachyonic instability within the horizon, instigating an exponential amplification of their amplitude [90].

By incorporating the above distinctive characteristic into specific inflationary scenarios, we can expect a PGW

interpretation of the PTA signal. In this paper, we consider two distinct scenarios: (1) the field ϕ acts as the inflaton while $S_{\rm other}$ represents a curvaton field, as illustrated in [90]; and (2) the field ϕ serves as the spectator field while $S_{\rm other}$ describes an inflaton.

For the first scenario, we postulate that the inflaton ϕ is endowed with Starobinsky's linear potential, expressed as [98],

$$V(\phi) = \begin{cases} V_0 + A_+(\phi - \phi_0), & \text{for } \phi > \phi_0, \\ V_0 + A_-(\phi - \phi_0), & \text{for } \phi \le \phi_0, \end{cases} \tag{4}$$

depicted in the top panel of Fig. 1. Here, V_0 determines the inflationary energy scale, while the parameters A_+ and A_- control the slopes of two linear potentials. The amplification of the small-scale primordial scalar spectrum, along with the formation of primordial black holes in the canonical single-field inflation with this potential, has been comprehensively investigated in [99]. However, in this paper, we can avoid discussing these phenomena due to the vanishing perturbations in the ϕ field.

For the second scenario, we choose the axion potential [100] to describe the field ϕ, which is given by

$$V(\phi) = \frac{1}{2}m^2\phi^2 + \Lambda^4\frac{\phi}{\sigma}\sin\left(\frac{\phi}{\sigma}\right), \tag{5}$$

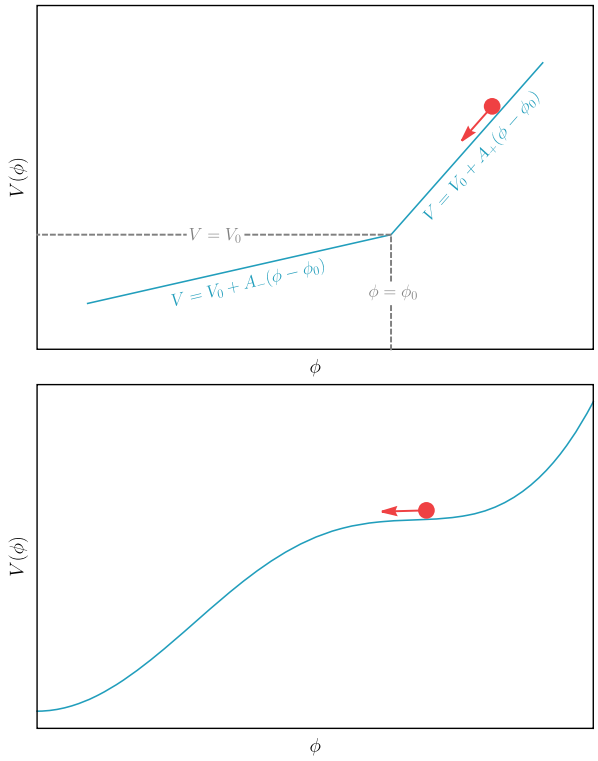

FIG. 1. Schematic diagrams of the Starobinsky's linear potential (top) and the axion potential (bottom).

as shown in the bottom panel of Fig. 1. This choice is the same as in [90], but the difference lies in our treatment of the field ϕ as a spectator field rather than as the inflaton. In the following section, we will explore the phenomenological implications of combining the NYmTG model with these two inflationary paradigms.

III. RESULTS

We perform numerical analyses to extract the PGW predictions arising from the NYmTG model within the previously mentioned inflationary contexts. By numerically solving the coupled set of background equations given in Eq. (2) and the tensor perturbation equation presented in Eq. (3), we can obtain the power spectrum of the tensor perturbations, $\mathcal{P}_h(k) = \sum_{A=R,L} k^3|h_k^A|/(2\pi^2)$. Subsequently, we deduce the current energy spectrum of PGWs through the correlation:

$$\Omega_{\rm GW}(k)h^2 = 6.8 \times 10^{-7}\mathcal{P}_h(k). \tag{6}$$

A. Starobinsky's linear potential

In this instance, the inflationary energy scale remains elusive, given that the curvaton field plays a role in the generation of primordial scalar perturbations. Consequently, V_0 emerges as a somewhat unconstrained parameter. To effectively explain the PTA signal through PGWs, we select the following parameters: $V_0 = 10^{-14}$, $A_+/V_0 = 1$, $A_-/A_+ = 0.1$, $\phi_0 = 6$, and $\alpha = 27$. Additionally, we designate the field value of ϕ at the moment when the CMB scale $k_{\rm CMB} = 0.05\ {\rm Mpc}^{-1}$ exits the horizon to be 11.32. Moreover, we define the e-folding number from the time when $\phi = 11.32$ to the end of inflation to be 60.

In Fig. 2, we depict the trajectory of the ϕ field velocity in relation to the e-folding number N. At the outset, the inflaton ϕ slowly rolls down along the potential's segment where $\phi > \phi_0$, with its velocity seeing a steady uptick, culminating around $N = 40$. Subsequently, the ϕ field

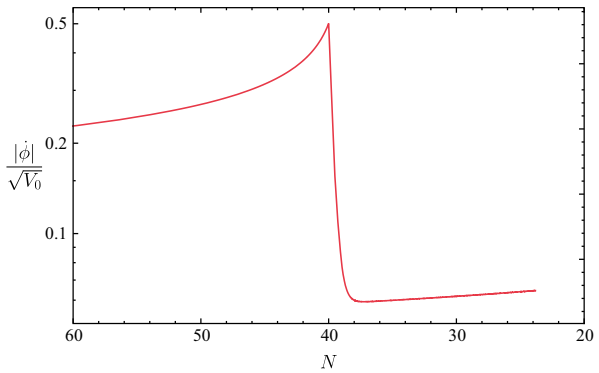

FIG. 2. The evolution of $|\dot{\phi}|/\sqrt{V_0}$ as a function of the e-folding number $N \equiv \ln(a_{\rm e}/a)$, with $a_{\rm e}$ being the scale factor at the end of inflation, in the first scenario.

crosses the point at $\phi = \phi_0$, transitioning onto the flatter segment of the potential where $\phi < \phi_0$. In the process, the inflaton velocity declines sharply, settling into a new slow-roll regime characterized by the smaller velocity. Consequently, the trajectory of the inflaton velocity prominently features a sharp peak, manifesting itself around $N = 40$.

Taking a closer look at Eq. (3), it is evident that when $\dot{\phi} < 0$ and $\alpha > 0$, the right-handed polarization state for tensor perturbations undergoes tachyonic instability. This instability translates to an exponential growth of the modes with right-handed polarization. However, this is not a uniform growth for all modes. Modes that exit the horizon at varying times will witness different levels of this instability, precisely because the strength of the tachyonic instability experienced by the modes is directly proportional to $|\alpha\dot{\phi}|$ evolving over time. Therefore, those modes that exit the horizon around the moment when $|\alpha\dot{\phi}|$ is at its largest will encounter the most pronounced amplification.

In light of the inflationary dynamics delineated in Fig. 2, the energy spectrum of the resulting PGWs exhibits a pinnacle, involving the contribution of only right-handed polarization state, in the vicinity of $\mathcal{O}(10^{-8})$ Hz, as discerned from Fig. 3. From this illustration, it becomes lucidly clear that the forecasted PGW signal coincides with the observational results from NANOGrav and EPTA. It is important to emphasize that selecting the parameters A_+ and A_- is critical in deriving a PGW signal that accounts for the PTA results. To demonstrate the sensitivity of the PTA signal explanation to variations in A_+ and A_-, we take the previously chosen parameters as the fiducial parameter set, and then we depict the current PGW energy spectra for the variations of A_+ and A_- by a factor of 1 ± 10^{-1} in Fig. 3. The results indicate that shifts in A_+ of 1 ± 10^{-1} have some

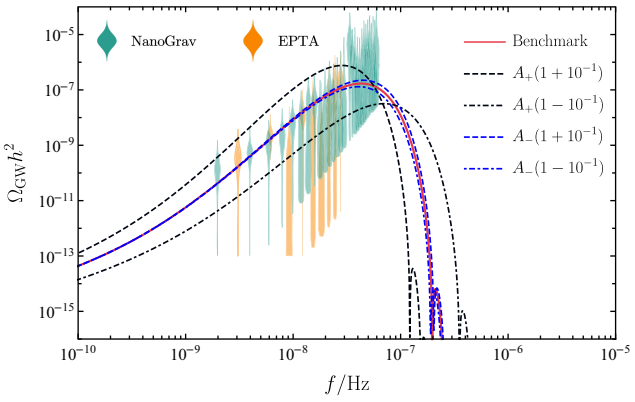

FIG. 3. The current energy spectrum of PGWs (red line) predicted by the NYmTG model within the first inflationary scenario. The violin diagrams depict the free spectrum posteriors in the analyses from the NANOGrav 15-yr dataset [58] and EPTA DR2 [101]. Also shown are the current energy spectra of PGWs for the variations in A_+ and A_- by a factor of 1 ± 10^{-1}, in comparison to the fiducial parameter set, which is associated with the red line.

effect on the peak position and amplitude of the energy spectrum, however, the resulting PGW signal remains consistent with the observational results. In comparison to the parameter A_+, the influence of variations in A_- by 1 ± 10^{-1} on the energy spectrum is relatively minor. On the whole, the PTA signal explanation exhibits relatively low sensitivity to variations in the parameters A_+ and A_-.

Intriguingly, even when considering large scales, the tensor modes with right-handed polarization exhibit distinct variations, setting them apart from their left-handed counterpart. As illustrated in Fig. 4, the large-scale tensor perturbations are characterized by a pronounced blue spectrum, within the current upper limit of $r < 0.036$. More importantly, the CMB-scale PGW signal, predominantly governed by the right-handed polarization state, is nearly exclusively right-handed in its polarization. Such chiral PGWs not only yield the B-mode (BB) autocorrelation spectrum but also result in nozero cross-correlation spectra between the CMB temperature and B-mode (TB), as well as between E-mode and B-mode (EB). The contributions from the PGWs to them are written as [102,103]

$$C_\ell^{BB} = 4\pi \int d(\ln k)[\mathcal{P}_h^L(k) + \mathcal{P}_h^R(k)]\Delta_\ell^B(k)\Delta_\ell^B(k),$$
$$C_\ell^{XB} = 4\pi \int d(\ln k)[\mathcal{P}_h^L(k) - \mathcal{P}_h^R(k)]\Delta_\ell^X(k)\Delta_\ell^B(k), \qquad (7)$$

where $X = \{T, E\}$ and $\Delta_\ell^{T/E/B}(k)$ is the radiation transfer function for $T/E/B$. In Fig. 5, we present the corresponding BB, EB, and TB spectra, $D_\ell^{XY} = \ell(\ell+1)C_\ell^{XY}/(2\pi)$ with $XY = \{BB, EB, TB\}$, derived by using the publicly available Boltzmann code CLASS [104]. Notably, the BB spectrum appears detectable by forthcoming CMB experiments, such as the LiteBIRD satellite [105]. A detection of the TB

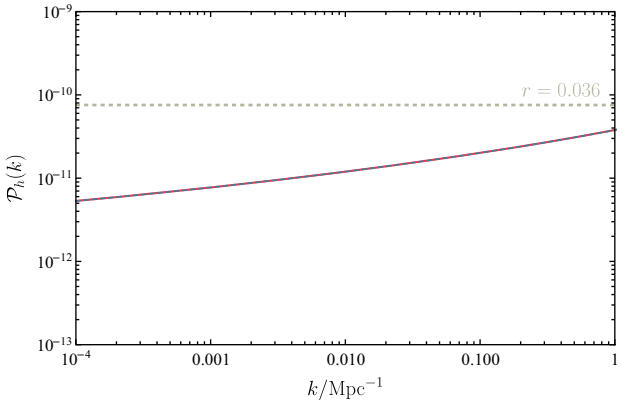

FIG. 4. The large-scale power spectrum of the tensor perturbations predicted by the NYmTG model within the first inflationary scenario. The solid line denotes the total power spectrum $\mathcal{P}_h(k)$, while the dashed line represents the power spectrum for the right-handed polarization. The scale-invariant tensor spectrum with $r = 0.036$ (gray dashed line) is shown as a reference.

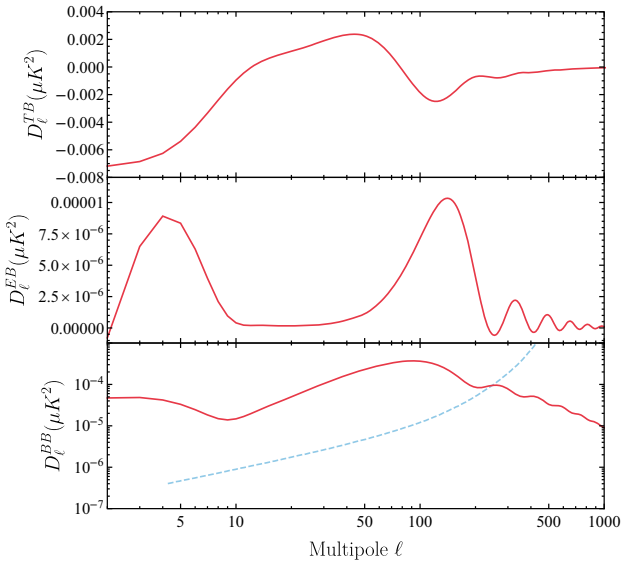

FIG. 5. The resulting CMB angular power spectra, $D_\ell^{XY} = \ell(\ell+1)C_\ell^{XY}/(2\pi)$ with $XY = \{BB, EB, TB\}$, expected due to the chiral tensor spectrum depicted in Fig. 4. The dashed line in the lower panel represents the expected sensitivity curve of the LiteBIRD mission [105].

and EB correlations would provide a strong evidence for our scenario.

B. Axion potential

In this setting, the action $S_{\rm other}$ delineates a canonical and minimally coupled inflaton, denoted by φ. For convenience, we adopt the Starobinsky potential, $V(\varphi) = V_0[1-\exp(-\sqrt{2/3}\varphi)]^2$ with $V_0 = 9.75\times10^{-11}$, serving as an emblematic example to illustrate the results within this scenario. We opt for an initial field value of the inflaton, $\varphi = 5.42$, corresponding the time when the scale $k_{\rm CMB}$ exits the horizon and ensuring that the inflation endures for a span of 60 e-folds. The parameters inherent to the potential, as expressed in Eq. (5), are selected as follows: $m = \sqrt{0.16V_0}$, $\sigma = 0.0002$, and $\beta \equiv \Lambda^4/(m^2\sigma^2) = 0.93$. Furthermore, we take $\alpha = 1.33\times10^5$, and the initial field value of the ϕ field, denoted by $\phi_{\rm ini}$, is chosen to be $\phi_{\rm ini} = \phi_0 = 6.612\times10^{-4}$. In this model, the potential exhibits a very flat region at $\phi_{\rm ini}$, which makes the rolling-down time of ϕ highly sensitive to the initial value $\phi_{\rm ini}$. Since quantum fluctuations of ϕ can be treated as a difference in $\phi_{\rm ini}$ across different large-scale regions, which results in the difference in the rolling-down time and a shift of the GW peak frequency. These fluctuations can be estimated as $H_{\rm inf}/(2\pi)$, which typically has a value of 10^{-7} for GUT scale inflationary models. We choose the parameters to ensure that the difference of 10^{-7} in $\phi_{\rm ini}$ can significantly affect the rolling-down time.

Analogous to the outcomes in the previous scenario, Fig. 6 unmistakably reveals a pronounced peak in the profile of $|\dot\phi|$ approximately at $N = 40$, attributed to the swift descent of the ϕ field over the cliff-like region of its potential during this brief period. Consequently, the forecasted chiral PGW signal emerges as a plausible explanation of the PTA results, as seen from Fig. 7. In this figure, we also show the current PGW energy spectra for the variations in σ and β by a factor of 1 ± 10^{-3}. The results suggest that shifts in σ of 1 ± 10^{-3} have some effect on the peak position of the energy spectrum and a negligible effect on the peak amplitude of the energy spectrum. A similar observation applies to the parameter β. Relative to the first inflationary scenario, the PTA signal explanation in the second inflationary scenario shows greater sensitivity to variations in the potential parameters.

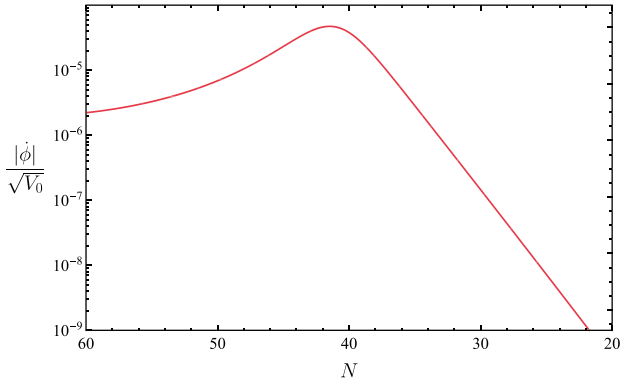

FIG. 6. The evolution of $|\dot\phi|/\sqrt{V_0}$ as a function of the e-folding number N in the second scenario.

The characteristic of this scenario is generating large anisotropies in the SGWB, allowing the PTA experiments to detect the GW polarization. Because of the poor angular resolution of the GW observers, we only focus on the large-scale perturbations in GW energy density which correspond to the low-ℓ region of the anisotropies. In this case, quantum fluctuations of ϕ in the first several e-foldings

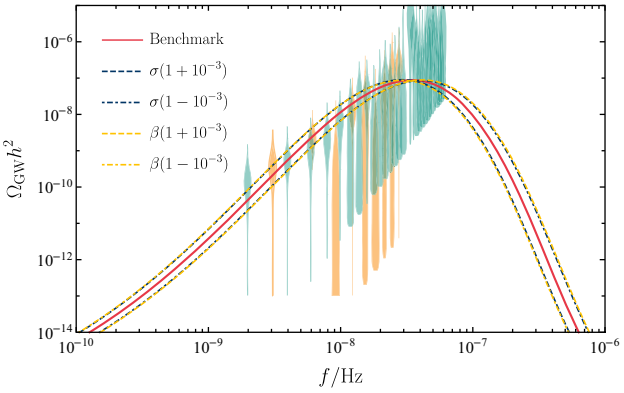

FIG. 7. The current energy spectrum of PGWs (red line) predicted by the NYmTG model within the second inflationary scenario. Also shown are the current energy spectra of PGWs for the variations in σ and β by a factor of 1 ± 10^{-3}, in comparison to the fiducial parameter set, which is associated with the red line.

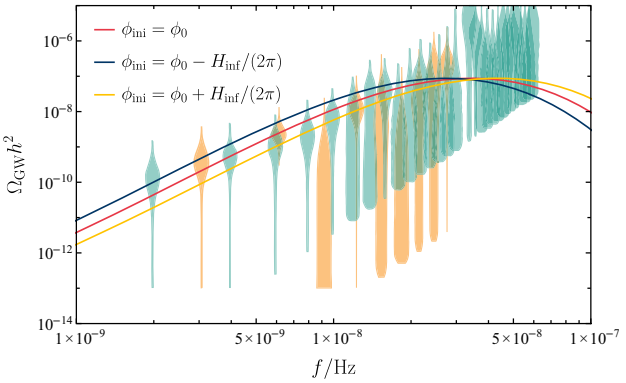

FIG. 8. The current energy spectra of PGWs under selecting different initial field values, $\phi_{\rm ini}=\phi_0$ and $\phi_{\rm ini}=\phi_0\pm H_{\rm inf}/(2\pi)$, with $H_{\rm inf}$ denoting the Hubble parameter during inflation.

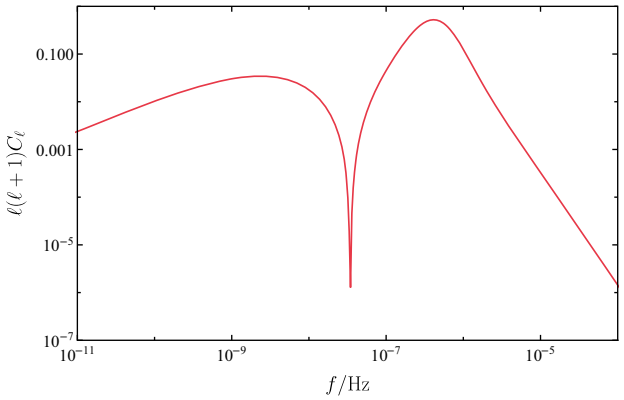

FIG. 9. The frequency-dependent angular power spectrum predicted by the axion potential.

of inflation result in large-scale inhomogeneous distribution of ϕ. Since ϕ is frozen on the potential at the beginning, $|\frac{\dot{\phi}}{H_{\rm inf}\phi_{\rm ini}}|\ll 1$ ($H_{\rm inf}$ denotes the Hubble parameter during inflation), superhorizon perturbations of ϕ remain almost constant until ϕ rolls down the potential. Also, superhorizon perturbations of ϕ can be treated as "initial value" of the dynamics of ϕ. As a consequence, in each large-scale region, the equivalent initial value of ϕ is different from each other by a quantity of the order of $H_{\rm inf}/(2\pi)$. Given the diminutive initial field value of ϕ, even small fluctuations in ϕ can result in non-negligible difference of the time when the ϕ field traverses the clifflike region in its potential. Since the peak value of amplified GWs is sensitive to this particular time, the averaged GW energy spectrum in each large-scale region differs with a shift in frequency.

In Fig. 8, we present the resulting GW energy spectra with different initial field values to demonstrate the mechanism of generating anisotropies, where the blue and yellow lines show $\Omega_{\rm GW}$ with $\phi_{\rm ini}=\phi_0\pm H_{\rm inf}/(2\pi)$ as comparisons to the averaged case with $\phi_{\rm ini}=\phi_0$. Figure 8 implies that the initial value from large-scale fluctuations of ϕ result in a frequency shift of $\Omega_{\rm GW}$. As a consequence, the value of $\Omega_{\rm GW}$ averaged in each large-scale region changes with $\phi_{\rm ini}$, i.e., anisotropies of the SGWB. Note that the anisotropies is also a frequency-dependent variable. We use the angular power spectrum to quantize the anisotropies. Similar to the Sachs-Wolfe plateau of CMB temperature perturbations for small multiple ℓ [106], we obtain

$$\ell(\ell+1)C_\ell(f)=\frac{\pi}{2}\langle\delta\Omega^2_{\rm GW}(f,\mathbf{x})\rangle. \tag{8}$$

Here, $\delta\Omega_{\rm GW}(f,\mathbf{x})\equiv(\Omega_{\rm GW}(f,\mathbf{x})-\overline{\Omega_{\rm GW}}(f))/\overline{\Omega_{\rm GW}}(f)$ denotes the spatial inhomogeneity of the GW energy spectrum, $\overline{\Omega_{\rm GW}}(f)$ is the averaged GW energy spectrum over the whole space, and the angle bracket denotes the power spectrum. Note that Eq. (8) is valid for any small ℓ. As we mentioned before, the angular power spectrum depends on the frequency f, which is shown in Fig. 9. The frequency-dependent angular power spectrum of order $\mathcal{O}(0.1)$ is a distinct feature to be verified by PTA observations in the near future [107–114]. Particularly, Ref. [112] points out that the angular power spectrum of $\mathcal{O}(0.1)$ with $\ell=1$ are expected to be observed by NANOGrav within 20 years. Moreover, the polarization of the SGWB can be measured by the PTA experiments thanks to the large anisotropies.

IV. CONCLUSION AND DISCUSSION

In this work, we examine the potential interpretation of the recently detected signal by PTA observations as the PGWs stemming from inflation within a parity-violating gravity model known as the NYmTG model. This model violates the parity symmetry in gravity by introducing the scalar field coupled Nieh-Yan term into teleparallel equivalent of general relativity, equivalently making a parity-violating extension to GR. Within the framework of the NYmTG model, we evaluate two distinct inflationary scenarios: in one, the coupled scalar field serves as an inflaton with Starobinsky's linear potential, while in the other, it acts as a spectator field governed by an axion potential. Both scenarios lead to a significant amplification of right-handed polarized tensor perturbations at certain scales, predicting a chiral PGW signal that coincides with the results from the PTA observations. Furthermore, our results reveal that the predicted PGWs manifest distinct characteristics: for the former scenario, strong circular polarization is evident at large scales, resulting in the nonzero TB and EB spectra; for the latter scenario, significant anisotropies emerge in PTA frequency band, rendering the polarization detectable through PTA experiments. With further experimental improvements, these features would become observable, offering compelling

evidence for our scenarios. Such observations promise to shed light on both the inflationary dynamics and the underlying gravity theory.

ACKNOWLEDGMENTS

We thank Zu-Cheng Chen and Lang Liu for fruitful discussions. This work is supported by the National Key Research and Development Program of China Grant No. 2020YFC2201502, the National Natural Science Foundation of China Grants No. 12305057, No. 12105060, No. 12147103, No. 12235019, No. 12075297 and No. 12147103, in part by the Science Research Grants from the China Manned Space Project with NO. CMS-CSST-2021-B01, in part by the Fundamental Research Funds for the Central Universities. X. Y. Y. is supported in part by the KIAS Individual Grant QP090701.

[1] P. A. R. Ade *et al.* (BICEP and Keck Collaborations), Improved constraints on primordial gravitational waves using Planck, WMAP, and BICEP/Keck observations through the 2018 observing season, Phys. Rev. Lett. **127**, 151301 (2021).
[2] R. Abbott *et al.* (KAGRA, Virgo, and LIGO Scientific Collaborations), Upper limits on the isotropic gravitational-wave background from Advanced LIGO and Advanced Virgo's third observing run, Phys. Rev. D **104**, 022004 (2021).
[3] E. Barausse *et al.*, Prospects for fundamental physics with LISA, Gen. Relativ. Gravit. **52**, 81 (2020).
[4] W.-H. Ruan, Z.-K. Guo, R.-G. Cai, and Y.-Z. Zhang, Taiji program: Gravitational-wave sources, Int. J. Mod. Phys. A **35**, 2050075 (2020).
[5] J. Luo *et al.* (TianQin Collaboration), TianQin: A space-borne gravitational wave detector, Classical Quantum Gravity **33**, 035010 (2016).
[6] G. Agazie *et al.* (NANOGrav Collaboration), The NANOGrav 15 yr data set: Evidence for a gravitational-wave background, Astrophys. J. Lett. **951**, L8 (2023).
[7] D. J. Reardon *et al.*, Search for an isotropic gravitational-wave background with the parkes pulsar timing array, Astrophys. J. Lett. **951**, L6 (2023).
[8] J. Antoniadis *et al.* (EPTA Collaboration), The second data release from the European pulsar timing array III. Search for gravitational wave signals, Astron. Astrophys. **678**, A50 (2023).
[9] H. Xu *et al.*, Searching for the nano-Hertz stochastic gravitational wave background with the Chinese pulsar timing array data release I, Res. Astron. Astrophys. **23**, 075024 (2023).
[10] G. Agazie *et al.* (NANOGrav Collaborations), The NANOGrav 15 yr data set: Constraints on supermassive black hole binaries from the gravitational-wave background, Astrophys. J. Lett. **952**, L37 (2023).
[11] J. Ellis, M. Fairbairn, G. Hütsi, J. Raidal, J. Urrutia, V. Vaskonen, and H. Veermäe, Gravitational waves from SMBH binaries in light of the NANOGrav 15-year data, Phys. Rev. D **109**, L021302 (2024).
[12] Y.-C. Bi, Y.-M. Wu, Z.-C. Chen, and Q.-G. Huang, Implications for the supermassive black hole binaries from the NANOGrav 15-year data set, Sci. China Phys. Mech. Astron. **66**, 120402 (2023).
[13] E. Cannizzaro, G. Franciolini, and P. Pani, Novel tests of gravity using nano-Hertz stochastic gravitational-wave background signals, arXiv:2307.11665.
[14] N. Bartolo *et al.*, Science with the space-based interferometer LISA. IV: Probing inflation with gravitational waves, J. Cosmol. Astropart. Phys. 12 (2016) 026.
[15] M. Mylova, O. Özsoy, S. Parameswaran, G. Tasinato, and I. Zavala, A new mechanism to enhance primordial tensor fluctuations in single field inflation, J. Cosmol. Astropart. Phys. 12 (2018) 024.
[16] S. D. Odintsov, V. K. Oikonomou, and F. P. Fronimos, Quantitative predictions for f(R) gravity primordial gravitational waves, Phys. Dark Universe **35**, 100950 (2022).
[17] V. K. Oikonomou, Amplification of the primordial gravitational waves energy spectrum by a kinetic scalar in $F(R)$ gravity, Astropart. Phys. **144**, 102777 (2023).
[18] T. Zhu, W. Zhao, and A. Wang, Polarized primordial gravitational waves in spatial covariant gravities, Phys. Rev. D **107**, 024031 (2023).
[19] L. Sorbo, Parity violation in the cosmic microwave background from a pseudoscalar inflaton, J. Cosmol. Astropart. Phys. 06 (2011) 003.
[20] J. L. Cook and L. Sorbo, Particle production during inflation and gravitational waves detectable by ground-based interferometers, Phys. Rev. D **85**, 023534 (2012); **86**, 069901(E) (2012).
[21] N. Barnaby, E. Pajer, and M. Peloso, Gauge field production in axion inflation: Consequences for monodromy, non-Gaussianity in the CMB, and gravitational waves at interferometers, Phys. Rev. D **85**, 023525 (2012).
[22] P. Adshead, E. Martinec, and M. Wyman, Gauge fields and inflation: Chiral gravitational waves, fluctuations, and the Lyth bound, Phys. Rev. D **88**, 021302 (2013).
[23] R. Namba, M. Peloso, M. Shiraishi, L. Sorbo, and C. Unal, Scale-dependent gravitational waves from a rolling axion, J. Cosmol. Astropart. Phys. 01 (2016) 041.
[24] V. Domcke, M. Pieroni, and P. Binétruy, Primordial gravitational waves for universality classes of pseudoscalar inflation, J. Cosmol. Astropart. Phys. 06 (2016) 031.
[25] M. Peloso, L. Sorbo, and C. Unal, Rolling axions during inflation: Perturbativity and signatures, J. Cosmol. Astropart. Phys. 09 (2016) 001.

[26] O. Özsoy and Z. Lalak, Primordial black holes as dark matter and gravitational waves from bumpy axion inflation, J. Cosmol. Astropart. Phys. 01 (2021) 040.
[27] G. D'Amico, N. Kaloper, and A. Westphal, Double monodromy inflation: A gravity waves factory for CMB-S4, LiteBIRD and LISA, Phys. Rev. D **104**, L081302 (2021).
[28] R.-G. Cai, C. Chen, and C. Fu, Primordial black holes and stochastic gravitational wave background from inflation with a noncanonical spectator field, Phys. Rev. D **104**, 083537 (2021).
[29] H. Di and Y. Gong, Primordial black holes and second order gravitational waves from ultra-slow-roll inflation, J. Cosmol. Astropart. Phys. 07 (2018) 007.
[30] R.-g. Cai, S. Pi, and M. Sasaki, Gravitational waves induced by non-Gaussian scalar perturbations, Phys. Rev. Lett. **122**, 201101 (2019).
[31] N. Bartolo, V. De Luca, G. Franciolini, A. Lewis, M. Peloso, and A. Riotto, Primordial black hole dark matter: LISA serendipity, Phys. Rev. Lett. **122**, 211301 (2019).
[32] K. Inomata and T. Nakama, Gravitational waves induced by scalar perturbations as probes of the small-scale primordial spectrum, Phys. Rev. D **99**, 043511 (2019).
[33] R.-G. Cai, S. Pi, S.-J. Wang, and X.-Y. Yang, Resonant multiple peaks in the induced gravitational waves, J. Cosmol. Astropart. Phys. 05 (2019) 013.
[34] Y.-F. Cai, C. Chen, X. Tong, D.-G. Wang, and S.-F. Yan, When primordial black holes from sound speed resonance meet a stochastic background of gravitational waves, Phys. Rev. D **100**, 043518 (2019).
[35] C. Yuan, Z.-C. Chen, and Q.-G. Huang, Probing primordial–black-hole dark matter with scalar induced gravitational waves, Phys. Rev. D **100**, 081301 (2019).
[36] C. Fu, P. Wu, and H. Yu, Primordial black holes from inflation with nonminimal derivative coupling, Phys. Rev. D **100**, 063532 (2019).
[37] C. Fu, P. Wu, and H. Yu, Scalar induced gravitational waves in inflation with gravitationally enhanced friction, Phys. Rev. D **101**, 023529 (2020).
[38] R.-G. Cai, Z.-K. Guo, J. Liu, L. Liu, and X.-Y. Yang, Primordial black holes and gravitational waves from parametric amplification of curvature perturbations, J. Cosmol. Astropart. Phys. 06 (2020) 013.
[39] J. Lin, Q. Gao, Y. Gong, Y. Lu, C. Zhang, and F. Zhang, Primordial black holes and secondary gravitational waves from k and G inflation, Phys. Rev. D **101**, 103515 (2020).
[40] S. Pi and M. Sasaki, Gravitational waves induced by scalar perturbations with a lognormal peak, J. Cosmol. Astropart. Phys. 09 (2020) 037.
[41] V. Vaskonen and H. Veermäe, Did NANOGrav see a signal from primordial black hole formation?, Phys. Rev. Lett. **126**, 051303 (2021).
[42] V. De Luca, G. Franciolini, and A. Riotto, NANOGrav data hints at primordial black holes as dark matter, Phys. Rev. Lett. **126**, 041303 (2021).
[43] K. Inomata, M. Kawasaki, K. Mukaida, and T. T. Yanagida, NANOGrav results and LIGO-Virgo primordial black holes in axionlike curvaton models, Phys. Rev. Lett. **126**, 131301 (2021).
[44] Z. Yi, Q. Gao, Y. Gong, and Z.-h. Zhu, Primordial black holes and scalar-induced secondary gravitational waves from inflationary models with a noncanonical kinetic term, Phys. Rev. D **103**, 063534 (2021).
[45] Q. Gao, Y. Gong, and Z. Yi, Primordial black holes and secondary gravitational waves from natural inflation, Nucl. Phys. **B969**, 115480 (2021).
[46] G. Domènech, Scalar induced gravitational waves review, Universe **7**, 398 (2021).
[47] M. Kamionkowski, A. Kosowsky, and M. S. Turner, Gravitational radiation from first order phase transitions, Phys. Rev. D **49**, 2837 (1994).
[48] C. Caprini, R. Durrer, and G. Servant, Gravitational wave generation from bubble collisions in first-order phase transitions: An analytic approach, Phys. Rev. D **77**, 124015 (2008).
[49] D. Cutting, M. Hindmarsh, and D. J. Weir, Gravitational waves from vacuum first-order phase transitions: From the envelope to the lattice, Phys. Rev. D **97**, 123513 (2018).
[50] M. Hindmarsh, S. J. Huber, K. Rummukainen, and D. J. Weir, Numerical simulations of acoustically generated gravitational waves at a first order phase transition, Phys. Rev. D **92**, 123009 (2015).
[51] H.-K. Guo, K. Sinha, D. Vagie, and G. White, Phase transitions in an expanding universe: Stochastic gravitational waves in standard and non-standard histories, J. Cosmol. Astropart. Phys. 01 (2021) 001.
[52] A. Vilenkin, Cosmic strings and domain walls, Phys. Rep. **121**, 263 (1985).
[53] T. Damour and A. Vilenkin, Gravitational wave bursts from cosmic strings, Phys. Rev. Lett. **85**, 3761 (2000).
[54] P. Auclair *et al.*, Probing the gravitational wave background from cosmic strings with LISA, J. Cosmol. Astropart. Phys. 04 (2020) 034.
[55] T. Hiramatsu, M. Kawasaki, and K. Saikawa, On the estimation of gravitational wave spectrum from cosmic domain walls, J. Cosmol. Astropart. Phys. 02 (2014) 031.
[56] K. Saikawa, A review of gravitational waves from cosmic domain walls, Universe **3**, 40 (2017).
[57] C. Caprini and D. G. Figueroa, Cosmological backgrounds of gravitational waves, Classical Quantum Gravity **35**, 163001 (2018).
[58] A. Afzal *et al.* (NANOGrav Collaborations), The NANOGrav 15 yr data set: Search for signals from new physics, Astrophys. J. Lett. **951**, L11 (2023).
[59] L. Bian, S. Ge, J. Shu, B. Wang, X.-Y. Yang, and J. Zong, Gravitational wave sources for pulsar timing arrays, arXiv:2307.02376.
[60] S. Vagnozzi, Inflationary interpretation of the stochastic gravitational wave background signal detected by pulsar timing array experiments, J. High Energy Astrophys. **39**, 81 (2023).
[61] G. Franciolini, A. Iovino, Jr., V. Vaskonen, and H. Veermae, The recent gravitational wave observation by pulsar timing arrays and primordial black holes: The importance of non-Gaussianities, Phys. Rev. Lett. **131**, 201401 (2023).
[62] V. K. Oikonomou, Flat energy spectrum of primordial gravitational waves versus peaks and the NANOGrav 2023 observation, Phys. Rev. D **108**, 043516 (2023).

[63] S. Wang, Z.-C. Zhao, J.-P. Li, and Q.-H. Zhu, Implications of pulsar timing array data for scalar-induced gravitational waves and primordial black holes: Primordial non-Gaussianity $f_{\rm NL}$ considered, arXiv:2307.00572.
[64] L. Liu, Z.-C. Chen, and Q.-G. Huang, Implications for the non-Gaussianity of curvature perturbation from pulsar timing arrays, arXiv:2307.01102.
[65] L. Liu, Z.-C. Chen, and Q.-G. Huang, Probing the equation of state of the early Universe with pulsar timing arrays, J. Cosmol. Astropart. Phys. 11 (2023) 071.
[66] C. Unal, A. Papageorgiou, and I. Obata, Axion-gauge dynamics during inflation as the origin of pulsar timing array signals and primordial black holes, arXiv:2307.02322.
[67] Y. Gouttenoire, First-order phase transition interpretation of PTA signal produces solar-mass black holes, Phys. Rev. Lett. **131**, 171404 (2023).
[68] S. A. Hosseini Mansoori, F. Felegray, A. Talebian, and M. Sami, PBHs and GWs from $\mathbb{T}^2$-inflation and NANOGrav 15-year data, J. Cosmol. Astropart. Phys. 08 (2023) 067.
[69] S. He, L. Li, S. Wang, and S.-J. Wang, Constraints on holographic QCD phase transitions from PTA observations, arXiv:2308.07257.
[70] J. Ellis, M. Fairbairn, G. Franciolini, G. Hütsi, A. Iovino, M. Lewicki, M. Raidal, J. Urrutia, V. Vaskonen, and H. Veermäe, What is the source of the PTA GW signal?, arXiv:2308.08546.
[71] Z. Yi, Z.-Q. You, Y. Wu, Z.-C. Chen, and L. Liu, Exploring the NANOGrav signal and planet-mass primordial black holes through Higgs inflation, arXiv:2308.14688.
[72] S. Choudhury, Single field inflation in the light of NANOGrav 15-year data: Quintessential interpretation of blue tilted tensor spectrum through non-bunch Davies initial condition, arXiv:2307.03249.
[73] S. Choudhury, A. Karde, S. Panda, and M. Sami, Scalar induced gravity waves from ultra slow-roll Galileon inflation, arXiv:2308.09273.
[74] G. Bhattacharya, S. Choudhury, K. Dey, S. Ghosh, A. Karde, and N. S. Mishra, Evading no-go for PBH formation and production of SIGWs using multiple sharp transitions in EFT of single field inflation, arXiv:2309.00973.
[75] R. Jackiw and S. Y. Pi, Chern-Simons modification of general relativity, Phys. Rev. D **68**, 104012 (2003).
[76] S. Alexander and N. Yunes, Chern-Simons modified general relativity, Phys. Rep. **480**, 1 (2009).
[77] A. Lue, L.-M. Wang, and M. Kamionkowski, Cosmological signature of new parity violating interactions, Phys. Rev. Lett. **83**, 1506 (1999).
[78] M. Satoh, S. Kanno, and J. Soda, Circular polarization of primordial gravitational waves in string-inspired inflationary cosmology, Phys. Rev. D **77**, 023526 (2008).
[79] S. H.-S. Alexander, M. E. Peskin, and M. M. Sheikh-Jabbari, Leptogenesis from gravity waves in models of inflation, Phys. Rev. Lett. **96**, 081301 (2006).
[80] S. H. S. Alexander, Inflationary birefringence and baryogenesis, Int. J. Mod. Phys. D **25**, 1640013 (2016).
[81] J. Qiao, T. Zhu, W. Zhao, and A. Wang, Polarized primordial gravitational waves in the ghost-free parity-violating gravity, Phys. Rev. D **101**, 043528 (2020).
[82] S. D. Odintsov and V. K. Oikonomou, Chirality of gravitational waves in Chern-Simons f(R) gravity cosmology, Phys. Rev. D **105**, 104054 (2022).
[83] M. Crisostomi, K. Noui, C. Charmousis, and D. Langlois, Beyond Lovelock gravity: Higher derivative metric theories, Phys. Rev. D **97**, 044034 (2018).
[84] X. Gao and X.-Y. Hong, Propagation of gravitational waves in a cosmological background, Phys. Rev. D **101**, 064057 (2020).
[85] T. Zhu, W. Zhao, and A. Wang, Gravitational wave constraints on spatial covariant gravities, Phys. Rev. D **107**, 044051 (2023).
[86] M. Li, H. Rao, and D. Zhao, A simple parity violating gravity model without ghost instability, J. Cosmol. Astropart. Phys. 11 (2020) 023.
[87] M. Li, H. Rao, and Y. Tong, Revisiting a parity violating gravity model without ghost instability: Local Lorentz covariance, Phys. Rev. D **104**, 084077 (2021).
[88] Q. Wu, T. Zhu, R. Niu, W. Zhao, and A. Wang, Constraints on the Nieh-Yan modified teleparallel gravity with gravitational waves, Phys. Rev. D **105**, 024035 (2022).
[89] F. Bombacigno, F. Moretti, S. Boudet, and G. J. Olmo, Landau damping for gravitational waves in parity-violating theories, J. Cosmol. Astropart. Phys. 02 (2023) 009.
[90] R.-G. Cai, C. Fu, and W.-W. Yu, Parity violation in stochastic gravitational wave background from inflation in Nieh-Yan modified teleparallel gravity, Phys. Rev. D **105**, 103520 (2022).
[91] J. Liu, L. Bian, R.-G. Cai, Z.-K. Guo, and S.-J. Wang, Constraining first-order phase transitions with curvature perturbations, Phys. Rev. Lett. **130**, 051001 (2023).
[92] N. Ramberg, W. Ratzinger, and P. Schwaller, One μ to rule them all: CMB spectral distortions can probe domain walls, cosmic strings and low scale phase transitions, J. Cosmol. Astropart. Phys. 02 (2023) 039.
[93] J. Liu, Distinguishing nanohertz gravitational wave sources through the observations of ultracompact minihalos, arXiv:2305.15100.
[94] R. Abbott *et al.* (LIGO Scientific, Virgo, and KAGRA Collaborations), Constraints on cosmic strings using data from the third Advanced LIGO–Virgo observing run, Phys. Rev. Lett. **126**, 241102 (2021).
[95] A. Romero, K. Martinovic, T. A. Callister, H.-K. Guo, M. Martínez, M. Sakellariadou, F.-W. Yang, and Y. Zhao, Implications for first-order cosmological phase transitions from the third LIGO-Virgo observing run, Phys. Rev. Lett. **126**, 151301 (2021).
[96] R. Kato and J. Soda, Probing circular polarization in stochastic gravitational wave background with pulsar timing arrays, Phys. Rev. D **93**, 062003 (2016).
[97] E. Belgacem and M. Kamionkowski, Chirality of the gravitational-wave background and pulsar-timing arrays, Phys. Rev. D **102**, 023004 (2020).
[98] A. A. Starobinsky, Spectrum of adiabatic perturbations in the universe when there are singularities in the inflation potential, JETP Lett. **55**, 489 (1992), https://ui.adsabs.harvard.edu/abs/1992JETPL..55..489S/abstract.
[99] S. Pi and J. Wang, Primordial black hole formation in Starobinsky's linear potential model, J. Cosmol. Astropart. Phys. 06 (2023) 018.

[100] T. Kobayashi, A. Oikawa, and H. Otsuka, New potentials for string axion inflation, Phys. Rev. D **93**, 083508 (2016).
[101] J. Antoniadis *et al.* (EPTA Collaborations), The second data release from the European pulsar timing array: V. Implications for massive black holes, dark matter and the early Universe, arXiv:2306.16227.
[102] S. Saito, K. Ichiki, and A. Taruya, Probing polarization states of primordial gravitational waves with CMB anisotropies, J. Cosmol. Astropart. Phys. 09 (2007) 002.
[103] V. Gluscevic and M. Kamionkowski, Testing parity-violating mechanisms with cosmic microwave background experiments, Phys. Rev. D **81**, 123529 (2010).
[104] J. Lesgourgues, The cosmic linear anisotropy solving system (CLASS) I: Overview, arXiv:1104.2932.
[105] H. Ishino *et al.*, LiteBIRD: Lite satellite for the study of B-mode polarization and inflation from cosmic microwave background radiation detection, Proc. SPIE Int. Soc. Opt. Eng. **9904**, 99040X (2016).
[106] A. R. Liddle and D. H. Lyth, *Cosmological Inflation and Large Scale Structure* (Cambridge University Press, Cambridge, 2000).
[107] S. R. Taylor and J. R. Gair, Searching for anisotropic gravitational-wave backgrounds using pulsar timing arrays, Phys. Rev. D **88**, 084001 (2013).
[108] C. M. F. Mingarelli, T. Sidery, I. Mandel, and A. Vecchio, Characterizing gravitational wave stochastic background anisotropy with pulsar timing arrays, Phys. Rev. D **88**, 062005 (2013).
[109] S. C. Hotinli, M. Kamionkowski, and A. H. Jaffe, The search for anisotropy in the gravitational-wave background with pulsar-timing arrays, Open J. Astrophys. **2**, 8 (2019).
[110] Y. Ali-Haïmoud, T. L. Smith, and C. M. F. Mingarelli, Fisher formalism for anisotropic gravitational-wave background searches with pulsar timing arrays, Phys. Rev. D **102**, 122005 (2020).
[111] Y. Ali-Haïmoud, T. L. Smith, and C. M. F. Mingarelli, Insights into searches for anisotropies in the nanohertz gravitational-wave background, Phys. Rev. D **103**, 042009 (2021).
[112] N. Pol, S. R. Taylor, and J. D. Romano, Forecasting pulsar timing array sensitivity to anisotropy in the stochastic gravitational wave background, Astrophys. J. **940**, 173 (2022).
[113] G. Agazie *et al.* (NANOGrav Collaborations), The NANOGrav 15 yr data set: Search for anisotropy in the gravitational-wave background, Astrophys. J. Lett. **956**, L3 (2023).
[114] G. Sato-Polito and M. Kamionkowski, Exploring the spectrum of stochastic gravitational-wave anisotropies with pulsar timing arrays, arXiv:2305.05690.